7-1-1993

Annealing Dynamics of Molecular-Beam Epitaxial GaAs Grown at 200°C

David C. Look
Wright State University - Main Campus, david.look@wright.edu

D. C. Walters

G. D. Robinson

J. R. Sizelove

M. G. Mier

See next page for additional authors

Annealing dynamics of molecular-beam epitaxial GaAs grown at 200 °C

D. C. Look, D. C. Walters, and G. D. Robinson
University Research Center, Wright State University, Dayton, Ohio 45435

J. R. Sizelove, M. G. Mier, and C. E. Stutz
Solid State Electronics Directorate, Wright Laboratory, WL/ELRA, Wright Patterson Air Force Base, Ohio 45433

(Received 2 July 1992; accepted for publication 18 March 1993)

By separating a 2-μm-thick molecular-beam-epitaxial GaAs layer grown at 200 °C from its 650-μm-thick substrate, we have been able to obtain accurate Hall-effect and conductivity data as functions of annealing temperature from 300 to 600 °C. At a measurement temperature of 300 K, analysis confirms that hopping conduction is much stronger than band conduction for all annealing temperatures. However, at higher measurement temperatures (up to 500 K), the band conduction becomes comparable, and a detailed analysis yields the donor and acceptor concentrations and the donor activation energy. Also, an independent absorption study yields the total and charged As_{Ga} concentrations. Comparisons of all of these quantities as a function of annealing temperature T_A show a new feature of the annealing dynamics, namely, that the dominant acceptor (probably V_{Ga} related) strongly decreases and then increases as T_A is increased from 350 to 450 °C. Above 450 °C, N_D, N_A, and $[As_{Ga}]$ all decrease, as is known from previous studies.

I. INTRODUCTION

GaAs grown at 200 °C has proven to be a very useful material, e.g., as a buffer layer or passivation layer for metal/semiconductor field-effect transistors (MESFETs), as a gate-insulator layer for metal/insulator FETs (MISFETs), and as the active layer for fast photoconductive switches.[1] In some of these cases, world-record performance has been demonstrated. Thus, it is essential to understand the electrical and optical properties of this material. Also, since many of the applications require annealing at temperatures up to 600 °C, it is important to understand the annealing dynamics. In this work, we use the Hall-effect and absorption techniques to study the annealing process. Together these methods provide some new insight into the behavior of the donor and acceptor defects, which are present at very high concentrations (10^{18}–10^{20} cm^{-3}) and control the optical and electrical properties.

II. SAMPLE GROWTH AND PREPARATION

The molecular-beam-epitaxial (MBE) layer was grown at 200 °C on a 2-in.-diam semi-insulating (SI) substrate in a modified Varian 360 system, using an As_4/Ga beam-equivalent pressure of 20. The thickness (2 μm) was well calibrated by reflection high-energy electron-diffraction (RHEED) oscillations. The substrate was not In bonded and the 200 °C temperature was simply the reading on a thermocouple which sits in a position near the sample; however, the electrical and optical characteristics were quite similar to those of other samples that were In bonded. Layers grown at 200 °C are single crystal up to thicknesses of 2 μm.[2] Seven 6×6 mm^2 samples were cut from near the middle of the wafer, and each sample was annealed at a different temperature in the range 300–600 °C (50 °C increments). Annealing was carried out in a tube furnace under flowing N_2 gas for 10 min. During the anneal, the samples were covered with an undoped GaAs wafer to minimize As loss. Absorption measurements, discussed later, were performed on the annealed layers before they were removed from their respective substrates, because it is straightforward to correct for substrate absorption. However, for conductivity and Hall-effect measurements, it was necessary to remove the layers[3] because the sheet conductance $\sigma_\square$ of a layer grown at 200 °C is less than that of its substrate after a high-temperature (>500 °C) anneal and the quantity $R_\square\sigma_\square^2$ (used for calculation of the sheet Hall coefficient $R_\square$) is smaller for the layer than for the substrate under all conditions, even without annealing.[4] Thus, it is nearly impossible to get good Hall-effect measurements on low-temperature (LT) MBE GaAs layers without separating the layers from their substrates.[3,4] Although the substrate removal technique has been discussed elsewhere,[3] we summarize it here: (i) grow a 500–1000 Å AlAs layer between the substrate and LTMBE layer; (ii) epoxy the sample, layer down, to a piece of glass, about the same size as the sample (6×6 mm^2, in our case); (iii) lap the 650 μm substrate down to about 100 μm; (iv) polish down to about 50 μm; (v) use a reactive-ion etch, which stops on AlAs, to remove the remaining substrate; (vi) etch off the AlAs layer with HF acid. This process has a high yield ($>90\%$) and the resulting layer/glass structure is very robust.[3]

III. HALL-EFFECT MEASUREMENTS AND ANALYSIS

Indium contacts were placed on the corners of the samples with a soldering iron, but were not alloyed in order to avoid temperature-induced sample changes which could interfere with the annealing results. Nevertheless, the contacts were ohmic, as expected from earlier studies.[5] The samples were then mounted in a Dewar system which is designed for conductivity and Hall-effect measurements up

 0021-8979/93/74(1)/306/5/$6.00

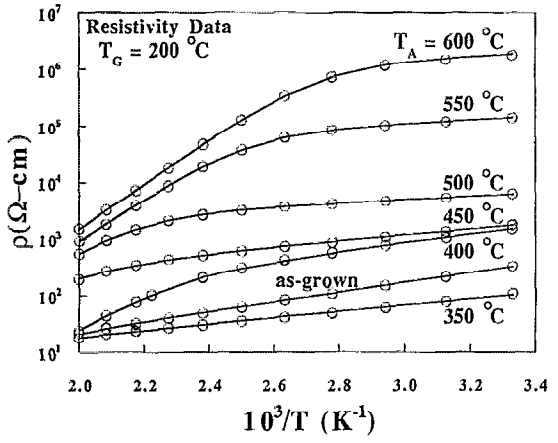

FIG. 1. Resistivity ρ vs inverse measurement temperature T^{-1} for various annealing temperatures T_A. The solid lines are theoretical fits.

to 600 K. Most of the data were taken in the range 300–500 K, the upper limit here being about the same as the growth temperature ($T_G \simeq 200$ °C). The resistivity and Hall-effect data for different annealing temperatures are presented in Figs. 1 and 2, respectively.

Analysis of the conductivity and Hall-effect data is complicated by the fact that two types of conductivity are present: band (b) conductivity, and hopping (h) conductivity. The latter results from the similar magnitudes of the donor (As_{Ga}) wave-function extent ($\sim$5–10 Å) and the average distance between donors ($\sim$13 Å for $N_D = 10^{20}$ cm^{-3}). For $T > 200$ K, the hopping is mostly between nearest neighbors, as shown earlier.[6] The relevant equations for the measured conductivity σ and Hall coefficient R are given below:[6,7]

$$\sigma_b = en_b\mu_b, \quad R_b = 1/en_b, \tag{1}$$

$$n_b = C_b[(N_D/N_A^{\rm net}) - 1]T^{3/2}e^{-E_{D0}/kT}, \tag{2}$$

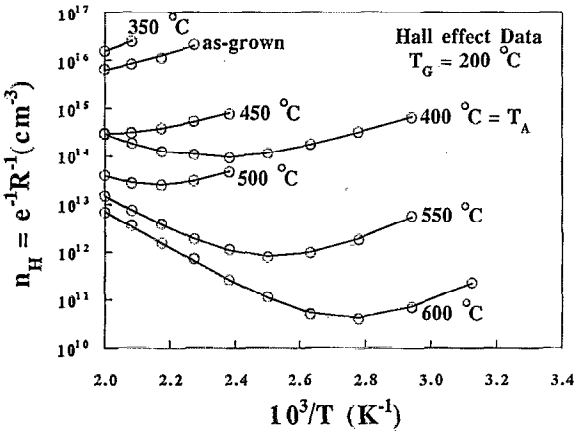

FIG. 2. Apparent carrier concentration n_H vs inverse measurement temperature T^{-1} for various annealing temperatures T_A. The solid lines are theoretical fits.

$$\mu_b^{-1} = \left(\frac{1}{8500(300/T)^{3/2}} + \frac{(2N_A+n)\ln(1+y)}{2.12\times10^{18}T^{3/2}}\right), \tag{3}$$

$$\sigma_h = C_h e^{-1.8/aN_D^{1/3}} e^{-bN_D^{1/3}/kT}, \tag{4}$$

$$\sigma = \sigma_b + \sigma_h, \tag{5}$$

$$R = \frac{R_b\sigma_b^2 + R_h\sigma_h^2}{(\sigma_b+\sigma_h)^2} \simeq \frac{R_b\sigma_b^2}{(\sigma_b+\sigma_h)^2}, \tag{6}$$

where $C_b = (g_0/g_1)N_C'e^{\beta/k}$, g_0/g_1 is a degeneracy factor, N_C' is the effective density of conduction-band states at $T = 1$ K, β is given by $E_D = E_{D0} - \beta T$, $y = 5.37\times10^8\ T^2/(2N_A+n)^{2/3}$, C_h is an unknown constant, $a = \hbar/(2m^*E_{D0})^{1/2}$, $b = C_1e^2/4\pi\epsilon$, and C_1 is a constant near unity. Equation (1) simply gives the definitions of the volume conductivity σ (not $\sigma_\square$) and Hall coefficient R, where the Hall r factor is assumed to be unity. Equation (2) gives the concentration n under the condition $n \ll N_A^{\rm net}$, certainly true in this case. Here, $N_A^{\rm net} = N_A - N_{DS}$, where N_{DS} represents all donors shallower than the dominant donor N_D. The constant C_b was fixed in the analysis at 7.56×10^{15} $cm^{-3}T^{-3/2}$, from assumed values $g_0/g_1 = 2$ (0/+ transition of a double donor such as EL2) and $\beta = 3.3\times10^{-4}$ eV/K (see Ref. 6). Equation (3) is a Matthiessen's rule addition of lattice and ionized-defect scattering. The lattice scattering (first term) is an empirical relationship which is of sufficient accuracy in the 300–500 K range (cf., e.g., Fig. 1.4.7 of Ref. 7), and the ionized-defect scattering is of the Conwell–Weisskopf form (Eq. 1.3.43, Ref. 7), applicable to semi-insulating samples. Equation (4) is a common representation of nearest-neighbor hopping conduction and is discussed in detail in Ref. 4. The constant 1.8 in Eq. (4) and the value of C_1 will vary according to a particular theoretical treatment, and the constant C_h should be dependent on N_D, N_A, and perhaps other factors, but not in a simple, generally accepted way. Thus, we have allowed C_1 and C_h to be fitting parameters as a function of annealing temperature T_A but not as a function of measurement temperature T. [The excellent fits of ρ vs T, Fig. 1, shows that the temperature dependence of Eq. (4) is entirely in the third factor.] As a function of T_A, $C_1 \simeq 3 \pm 1$, varying in a somewhat random fashion, whereas C_h varies strongly, decreasing monotonically as T_A increases. Thus, the factors C_h and $\exp(-1.8/aN_D^{1/3})$ should really be considered as a joint unknown in this case, reflecting the fact that the 1.8 and/or a factors are incorrect. Equations (5) and (6) simply display the additive relationships for σ and R when conduction is occurring in two bands,[7] and the second equality in Eq. (6) makes use of the fact that hopping conduction gives a vanishing (or unmeasurable) Hall coefficient. Clearly the measured R should be very small when $\sigma_h \gg \sigma_b$ and this is the case for much of the data, especially for low annealing temperature T_A and low measurement temperature T. For example, the unannealed sample has such a strong σ_h that a finite R cannot even be measured below 480 K. Obviously, the accuracy on N_A and E_{D0} is poorer in such cases.

Equations (1)–(6) were simultaneously fitted to σ vs T and R vs T data by a least-squares method. The fitted

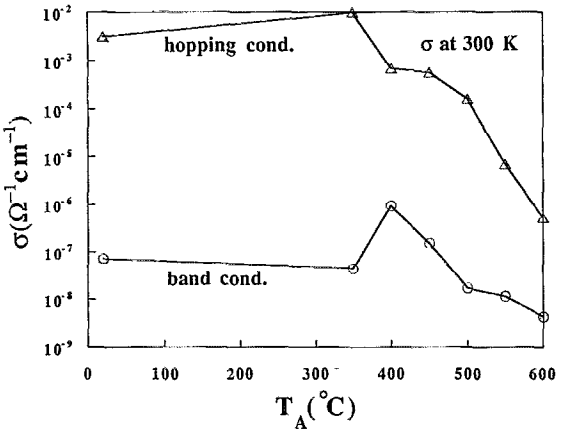

FIG. 3. The two components of conductivity σ (band and hopping) as functions of annealing temperature T_A.

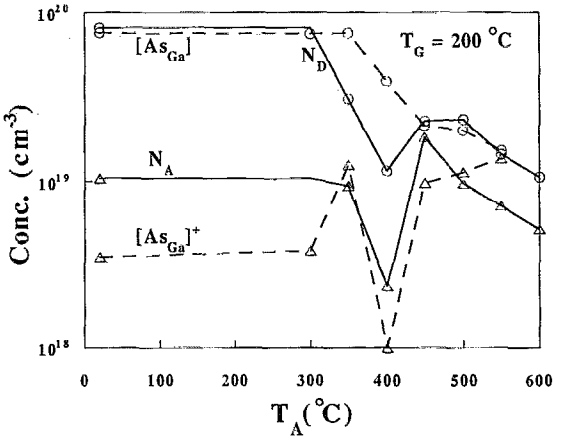

FIG. 5. The donor N_D, acceptor N_A, total antisite $[As_{Ga}]$, and charged antisite $[As_{Ga}]^+$ concentrations as functions of annealing temperature T_A.

parameters were N_D, N_A, E_{D0}, C_1, and C_h. The fits to the data are excellent, as evidenced by the solid lines in Figs. 1 and 2. Note that the hopping conduction measured at 300 K is much stronger than the band conduction for all annealing temperatures, as explicitly shown in Fig. 3; however, for 500 K measurements, the band conduction is stronger at the higher annealing temperatures ($T_A \geq 450$ °C), as can be indirectly determined from the positions of the minima in the n_H vs T^{-1} curves (Fig. 2). The fitted parameters E_{D0} and μ_b are presented in Fig. 4 and the parameters N_D and N_A in Fig. 5. All are discussed further below.

IV. ABSORPTION ANALYSIS

The EL2 photoionization cross sections σ_n and σ_p, representing the transitions $As^0_{Ga}+h\nu \rightarrow As^+_{Ga}+e^-$ and $As^+_{Ga}+h\nu \rightarrow As^0_{Ga}+h^+$, respectively, are well known as functions of $h\nu$.[8] (Here we have assumed that σ_n and σ_p for As_{Ga} are equivalent to their respective values for EL2.)

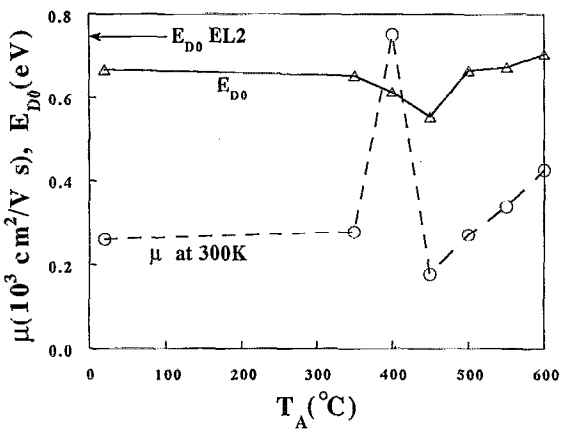

FIG. 4. The mobility μ and fitted activation energy E_{D0} as functions of annealing temperature T_A. Also noted is the literature value of E_{D0} for EL2.

For ease of analysis, it is more convenient to leave the layer l on the substrate s for the absorption measurements. Then the measured absorption coefficient α at wavelength λ is given by

$$\alpha(\lambda)d=\alpha_l(\lambda)d_l+\alpha_s(\lambda)d_s, \tag{7}$$

$$\alpha_l(\lambda)=\sigma_n(\lambda)[As_{Ga}]^0_l+\sigma_p(\lambda)[As_{Ga}]^+_l, \tag{8}$$

where d, d_l, and d_s are the total, layer, and substrate thicknesses, respectively. Since $\alpha_s d_s$ can be measured independently, by looking at a substrate without a layer, we can determine $[As_{Ga}]^0_l$ and $[As_{Ga}]^+_l$ by taking data at two different wavelengths (1.1 and 1.2 μm, in our case). The total $[As_{Ga}]$ (the sum of the neutral and charged components) and $[As_{Ga}]^+$ are plotted vs T_A in Fig. 5.

V. DISCUSSION

The annealing dependencies of the donor N_D and acceptor N_A concentrations, as deduced from the Hall-effect data, and the total antisite $[As_{Ga}]$ and charged antisite $[As_{Ga}]^+$ concentrations, as determined from the absorption measurements, are presented in Fig. 5. The near equivalence of N_D and $[As_{Ga}]$, except in the region 300 °C $< T_A <$ 450 °C, is rather remarkable, since the Hall-effect and absorption experiments are totally independent of each other. Even N_A and $[As_{Ga}]^+$ are within a factor of 2 over the whole T_A range, although the accuracy of these two parameters is poorer than that of N_D and $[As_{Ga}]$. The prevailing model of annealing in LTMBE GaAs is that $[As_{Ga}]$ and $[As_{Ga}]^+$ (presumably N_A) begin to decrease at $T_A \sim 400$ °C, and fall an order of magnitude or more by $T_A = 600$ °C. However, our Hall-effect measurements of N_D and N_A show that the situation is more complex than this. That is, something unusual is happening in the range 350 °C $\leq T_A \leq$ 450 °C, as evidenced not only by the data in Fig. 5, but also by the raw data of Figs. 1 and 2, in which the 400 °C annealing curves are clearly out of place. This is not an isolated occurrence, but has been seen in other samples grown at 200 and 250 °C and annealed under similar conditions; however, in some cases the exact temperature

at which the anomaly occurs may differ by 25–50 °C. The phenomenon is also evidently not due to inhomogeneous distributions of N_D, N_A, or σ, because these parameters have proven to be laterally homogeneous on a 2-in.-diam wafer grown at 200 °C and also homogeneous in depth.[4] Thus, we believe that we are witnessing a phenomenon that is quite common to MBE GaAs layers grown at 200 °C.

Before discussing possible models, we should compare the present results with those of Ref. 6, in which the layers were not removed from their respective substrates. At that time it was recognized that the condition $\sigma_{\square l} \gg \sigma_{\square s}$ (l =layer, s=substrate) must hold for accurate conductance measurements, but not that the condition $R_{\square l}\sigma_{\square l}^2 \gg R_{\square s}\sigma_{\square s}^2$ was also necessary for accurate Hall-coefficient determinations. From Eq. (4) we see that N_D can be determined from σ alone, and indeed the values of N_D obtained in Ref. 6 agreed well with values determined by absorption measurements on the same samples. In fact, the N_D's in that work ($\approx 3\times 10^{19}$ cm^{-3} for the unannealed sample) are comparable to those in the present investigation ($\sim 8\times 10^{19}$ cm^{-3}) considering the somewhat different growth conditions involved. However, the Hall-effect determination of N_A comes only from Eqs. (2) and (3), which both depend upon the accurate measurement of R. As it turns out, the measured R's in Ref. 6 were coming mainly from the substrate, and the net effect was a value of N_A which was much too small (10^{15} instead of 10^{19} cm^{-3}). Also, the value of E_{D0} [Eq. (2)] was that of EL2 in the substrate, although the actual magnitude (0.75 eV) is only slightly larger than the E_{D0}'s measured in the present work, since both EL2 and the LTMBE donor are related to As_{Ga}. Thus, in Ref. 6, the determination of N_D was accurate, but that of N_A and E_{D0} poor, although E_{D0} turned out to be fortuitously close to the correct value as explained above. In any case, it is clear that substrate removal is absolutely essential for obtaining accurate values of many of the parameters. In general, we estimate that the present methodology can determine N_D and N_A to better than a factor of 2, and E_{D0} to about 5%.

We next discuss our data in terms of two possible models.

A. Model 1

In this model, we assume that only one donor is present, namely, an As_{Ga}-related center with an energy $E_{D0}\simeq 0.65$–0.70 eV. Then the approximately 0.1 eV drop in E_{D0} at T_A=400 and 450 °C (Fig. 4) is assumed to be only an aberration of the fitting process, as is the difference between N_D and $[As_{Ga}]$ at these two annealing temperatures (Fig. 5). In fact, for $N_A \ll N_D$, which is the case at T_A=400 °C, we might expect that Eq. (2) is invalid and should be replaced by one in which the effective activation energy moves toward $E_{D0}/2$.[7] However, we have also fitted the data with the exact n vs T relationship, and have found no significant differences in the fitting parameters. Furthermore, at T_A=450 °C, N_D and N_A are comparable, and still E_{D0} is well below 0.7 eV. Thus, the problems with model 1 are twofold: (i) For T_A=400 °C, the fitted N_D is a factor of 4 below the fitted $[As_{Ga}]$; and (ii) at T_A=450 °C, the fitted E_{D0} is about 0.1 eV below the average value of E_{D0} over the rest of the T_A range. However, we perhaps can argue that these problems are minor considering the complexities of the Hall-effect and absorption analyses.

B. Model 2

In this model, there are two donors, one near 0.7 eV ($N_{D,0.7}$) and the other near 0.5 eV ($N_{D,0.5}$). Indeed, there is already good evidence for the presence of a donor shallower than EL2.[9,10] The problem mentioned before, that $N_D < [As_{Ga}]$ at T_A=350 and 400 °C, is now easily explained by the fact that the Fermi level E_F has moved up closer to the shallower donor $N_{D,0.5}$ because of a decrease in N_A such that $N_A < N_{D,0.5}$. That is, in this model the fitted N_D is really $N_{D,0.5}$ rather than $N_{D,0.7}$ for T_A=350 and 400 °C. Also, we can explain the decrease in E_{D0} (Fig. 4) and the strong decrease in $[As_{Ga}]^+$ (because E_F has moved well above $E_C-0.7$ eV). The main problem, however, is that at T_A=450 °C, E_{D0} is at its lowest value (0.55 eV) so that we would expect $N_D \simeq N_{D,0.5}$, whereas in Fig. 5 we see that $N_D \simeq [As_{Ga}] \simeq N_{D,0.7}$. It is possible that this latter near equivalence is a coincidence, but if E_F is near $E_C-0.5$ eV, we would still expect that $[As_{Ga}]^+$ should be very small, and this is not the case, according to the data in Fig. 5.

Although we cannot judge absolutely the relative merits of models 1 and 2 at this time, they both include a very interesting feature of the dominant acceptor N_A, namely a strong decrease in the range $350 \leqslant T_A \leqslant 400$ °C, and a subsequent increase at $400 \leqslant T_A \leqslant 450$ °C. This decrease in N_A at 400 °C is confirmed by the decrease in $[As_{Ga}]^+$ (Fig. 5), the increase in mobility (Fig. 4), the increase in band conduction (Fig. 3), and the decrease in hopping conduction (Fig. 3). (The decrease in hopping conduction results, at least in part, because there are fewer holes in the donor band to promote hopping.) It is likely that N_A is related to V_{Ga}, because that is the only acceptor point defect expected to exist in large concentrations in strongly As-rich materials. A possible scenario is that the As interstitials (or dimers) begin to move at about 350 °C and collide with the V_{Ga} (because there is a Coulombic attraction), forming As_iV_{Ga}, or As_{Ga}, or possibly a complex of As_{Ga} if the V_{Ga} were initially complexed. Another possibility is that the V_{Ga} themselves move. (Note that 1 MeV electron irradiation damage in GaAs, which includes vacancy production, mainly anneals in a stage around 300 °C.) In either case, N_A decreases. Then, from 400 to 450 °C, the new center breaks up, again forming V_{Ga} or a complex involving V_{Ga}. At these temperatures, even the original As_{Ga} centers begin to disappear and As precipitates are formed. This process must involve the reaction $As_{Ga} \rightarrow As_i + V_{Ga}$ which could give an excess of V_{Ga} (or N_A) even above the original concentration, as is apparently observed in Fig. 5 at T_A =450 °C. Then, above 450 °C, the V_{Ga} begin to find sinks, and N_A steadily decreases.

Although this model is unconfirmed, it does fit most of our Hall-effect and absorption data and thus has some credibility. Further studies will be necessary to fully elucidate the annealing dynamics.

VI. SUMMARY

By separating the LTMBE layer from its substrate, we have been able to carry out accurate temperature-dependent Hall-effect and conductivity measurements as functions of annealing temperature. A comparison with the total and charged As_{Ga} concentrations, as deduced from absorption measurements, allows an annealing model to be formulated. Although the microscopic nature of the model is somewhat uncertain, a new feature is that the dominant acceptor (likely V_{Ga} related) strongly decreases for T_A between 350 and 400 °C, and then strongly increases from 400 to 450 °C. Other details of the annealing dynamics must await further study.

ACKNOWLEDGMENTS

We wish to thank T. A. Cooper for the electrical measurements, J. T. Prichard for the substrate removal, E. N. Taylor for the crystal growth, J. Stephenson for the graphics, and N. Blair for manuscript preparation. D.C.L., D.C.W., and G.D.R. were supported under USAF Contract No. F33615-91-C-1765 and all of the work was carried out in the Solid State Electronics Directorate, Wright Laboratory.

[1] F. W. Smith, Mater. Res. Soc. Symp. Proc. **241**, 3 (1992).
[2] Z. Liliental-Weber, W. Swider, K. M. Yu, J. Kortright, F. W. Smith, and A. R. Calawa, Appl. Phys. Lett. **58**, 2153 (1991).
[3] D. C. Look, G. D. Robinson, J. R. Sizelove, and C. E. Stutz, in *Semi-insulating III-V Materials*, Ixtapa, 1992, edited by C. J. Miner (Adam Hilger, Bristol, in press).
[4] D. C. Look, D. C. Walters, M. Mier, C. E. Stutz, and S. K. Brierley, Appl. Phys. Lett. **60**, 2900 (1992).
[5] H. Yamamoto, Z.-Q. Fang, and D. C. Look, Appl. Phys. Lett. **57**, 1537 (1990).
[6] D. C. Look, D. C. Walters, M. O. Manasreh, J. R. Sizelove, C. E. Stutz, and K. R. Evans, Phys. Rev. B **42**, 3578 (1990).
[7] D. C. Look, *Electrical Characterization of GaAs Materials and Devices* (Wiley, New York, 1989).
[8] P. Silverberg, P. Omling, and L. Samuelson, Appl. Phys. Lett. **52**, 1689 (1988).
[9] D. C. Look, J. E. Hoelscher, J. Grant, C. E. Stutz, K. R. Evans, and M. Numan, Mater. Res. Soc. Symp. Proc. **241**, 87 (1992).
[10] H. J. von Bardeleben, M. O. Manasreh, D. C. Look, K. R. Evans, and C. E. Stutz, Phys. Rev. B **45**, 3372 (1992).